NASA/CR-2010-216292

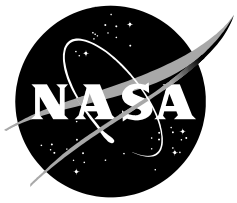

Objective Lightning Probability Forecasting for Kennedy Space Center and Cape Canaveral Air Force Station, Phase III

Winifred C. Crawford
ENSCO, Inc., Cocoa Beach, Florida
NASA Applied Meteorology Unit, Kennedy Space Center, Florida

October 2010

NASA STI Program ... in Profile

Since its founding, NASA has been dedicated to the advancement of aeronautics and space science. The NASA scientific and technical information (STI) program plays a key part in helping NASA maintain this important role.

The NASA STI program operates under the auspices of the Agency Chief Information Officer. It collects, organizes, provides for archiving, and disseminates NASA's STI. The NASA STI program provides access to the NASA Aeronautics and Space Database and its public interface, the NASA Technical Report Server, thus providing one of the largest collections of aeronautical and space science STI in the world. Results are published in both non-NASA channels and by NASA in the NASA STI Report Series, which includes the following report types:

- TECHNICAL PUBLICATION. Reports of completed research or a major significant phase of research that present the results of NASA Programs and include extensive data or theoretical analysis. Includes compilations of significant scientific and technical data and information deemed to be of continuing reference value. NASA counterpart of peer-reviewed formal professional papers but has less stringent limitations on manuscript length and extent of graphic presentations.

- TECHNICAL MEMORANDUM. Scientific and technical findings that are preliminary or of specialized interest, e.g., quick release reports, working papers, and bibliographies that contain minimal annotation. Does not contain extensive analysis.

- CONTRACTOR REPORT. Scientific and technical findings by NASA-sponsored contractors and grantees.

- CONFERENCE PUBLICATION. Collected papers from scientific and technical conferences, symposia, seminars, or other meetings sponsored or co-sponsored by NASA.

- SPECIAL PUBLICATION. Scientific, technical, or historical information from NASA programs, projects, and missions, often concerned with subjects having substantial public interest.

- TECHNICAL TRANSLATION. English-language translations of foreign scientific and technical material pertinent to NASA's mission.

Specialized services also include organizing and publishing research results, distributing specialized research announcements and feeds, providing help desk and personal search support, and enabling data exchange services.

For more information about the NASA STI program, see the following:

- Access the NASA STI program home page at *http://www.sti.nasa.gov*

- E-mail your question via the Internet to help@sti.nasa.gov

- Fax your question to the NASA STI Help Desk at 443-757-5803

- Phone the NASA STI Help Desk at 443-757-5802

- Write to:
  NASA STI Help Desk
  NASA Center for AeroSpace Information
  7115 Standard Drive
  Hanover, MD 21076-1320

NASA/CR-2010-216292

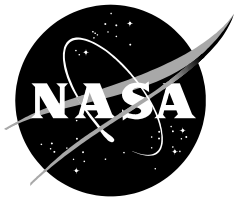

Objective Lightning Probability Forecasting for Kennedy Space Center and Cape Canaveral Air Force Station, Phase III

Winifred C. Crawford
ENSCO, Inc., Cocoa Beach, Florida
NASA Applied Meteorology Unit, Kennedy Space Center, Florida

National Aeronautics and
Space Administration

Kennedy Space Center
Kennedy Space Center, FL 32899-0001

October 2010

Acknowledgements

The author thanks Mr. William Roeder of the 45th Weather Squadron and Dr. Francis J. Merceret, the AMU Chief, for lending their statistical expertise to this project, and to Mr. Stephen Madison of Computer Sciences Raytheon for providing the data.

Available from:

NASA Center for AeroSpace Information
7115 Standard Drive
Hanover, MD 21076-1320
(443) 757-5802

This report is also available in electronic form at
http://science.ksc.nasa.gov/amu/final.html

Executive Summary

The 45th Weather Squadron (45 WS) includes the probability of lightning occurrence in their daily morning briefings. This forecast is important in the warm season months, May–September, when the area is most affected by lightning. This information is used by forecasters to assess the likelihood launch commit criteria and weather flight rules will be violated, and planning for daily ground operations on Kennedy Space Center and Cape Canaveral Air Force Station (CCAFS). The lightning probability forecast is based on the output from an objective lightning forecast tool developed by the Applied Meteorology Unit (AMU) that is supplemented by subjective analyses of model and observational data. This tool was developed over two phases. In Phase I, the AMU developed a set of equations that calculate the probability of lightning occurrence for the day that outperformed the previous operational tool by 48%, and a graphical user interface (GUI) to input the parameter values and display the output. In Phase II, the equations were redeveloped with new data, and the GUI transitioned to the Meteorological Interactive Data Display System (MIDDS). The MIDDS GUI retrieves the required predictor values automatically, reducing work load on the forecasters. The Phase II equations outperformed Phase I by 8%, for a total combined improvement in skill of 56%.

The success of the previous work led the 45 WS to task the AMU with Phase III to improve the tool further. The period of record was increased from 17 to 20 years (1989–2008), and data for October were included. The main goal was to create equations based on the progression of the lightning probabilities in the daily climatology instead of creating an equation for each warm season month. Five distinct sub-seasons can be discerned from the daily lightning climatology. An equation for each of these sub-seasons would be created under the assumption that they would capture the physical attributes that contribute to thunderstorm formation more so than monthly equations.

The data sources were the same as for Phase II and included the Cloud-to-Ground Lightning Surveillance System (CGLSS), 1200 UTC Florida synoptic soundings, and the 1000 UTC CCAFS sounding (XMR). Data from CGLSS were used to determine lightning occurrence for each day. The 1200 UTC Florida and 1000 UTC XMR soundings were used to determine the flow regime and the 1000 UTC XMR soundings were used to calculate local stability parameters for each day. These datasets were processed and analyzed to create the predictand and candidate predictors needed for the statistical forecast equation development. The CGLSS data were used to create a binary predictand for lightning: a ‘1’ for lightning occurrence during the day and a ‘0’ for non-occurrence. The flow regimes and stability parameters from the soundings were used to calculate the candidate predictors of lightning occurrence.

The AMU stratified the data into two sub-sets: a development dataset containing 16 warm seasons from which the equations were developed, and verification dataset of 4 warm seasons on which the equations were tested. Before the equations could be developed, they had to be stratified again into sub-seasons. The sub-season start dates were not expected to be identical in every year, therefore the AMU developed and tested three methods to determine the start dates in each year. The ground-truth for testing came from a set of historical wet-season start dates determined by the National Weather Service in Melbourne, Fla. None of the three methods were able to determine the actual start dates in each year, therefore, the start dates were specified by the daily climatology and were the same in every year.

The methods for developing and testing the equations were identical to those followed in Phase II. One logistic regression equation was developed for each sub-season, and the resulting five equations contained one to three predictors. The performance of these equations was compared to that of five other forecast method including the Phase II equations. The new equations outperformed every method except Phase II. Therefore, the Phase III equations will not replace the Phase II equations in operations. The reason for the degradation could be that the same sub-season start dates were used in every year. It is likely there was overlap of sub-season days at the beginning and end of each defined sub-season in each individual year, which could affect the predictors chosen, their coefficients in the logistic regression and, ultimately, equation performance. Future work should include an effort to create an objective method that determines the start dates of the sub-seasons in each individual year.

Table of Contents

List of Figures

List of Tables

1 Introduction

The 45th Weather Squadron (45 WS) forecasters include a probability of lightning occurrence in their daily 24-Hour and Weekly Planning forecasts, which are briefed to the 45 WS staff in the morning at 1100 UTC (0700 EDT) and released for customer use at 1130 UTC (0730 EDT). Forecasters at the Spaceflight Meteorology Group also make thunderstorm forecasts during shuttle operations. The probability of lightning occurrence is used by personnel in determining the possibility of violating launch commit criteria and shuttle weather flight rules, and planning for daily ground operation activities on Kennedy Space Center (KSC) and Cape Canaveral Air Force Station (CCAFS). This forecast is critically important in the warm season months, May–September, when the area is most affected by lightning.

The lightning probability forecast is based on the output from an objective lightning forecast tool developed by the Applied Meteorology Unit (AMU; Bauman et al. 2004) that is supplemented by subjective analyses of model and observational data. This tool was developed over two phases. In Phase I, the AMU developed five equations, one for each warm season month, that calculate the probability of lightning occurrence for the day (Lambert and Wheeler 2005) and a Microsoft® Excel© graphical user interface (GUI) to display the output. The GUI allowed forecasters to interface with the equations by entering predictor values to output a probability of lightning occurrence. In Phase II (Lambert 2007), the equations were redeveloped by using two more years of data and modified predictors, and the GUI was transitioned to the Meteorological Interactive Data Display System (MIDDS). The Phase I equations outperformed several forecast methods used in operations and the Phase II equations, in turn, outperformed the Phase I equations.

Based on the successes in the previous phases, the 45 WS tasked the AMU with Phase III to improve the tool further. Three warm seasons were added to increase the period of record (POR) to 20 years (1989–2008), and October data were included to capture the end of the lightning season. The main goal was to create equations based on the progression of the lightning season in the daily climatology instead of creating an equation for each warm season month. The assumption was that these equations would capture the physical attributes that contribute to thunderstorm formation more so than monthly equations.

1.1 Phases I and II

The Phase I objective lightning probability tool was a set of five logistic regression equations that calculated the probability of lightning occurrence for the day (Lambert and Wheeler 2005) in a rectangular area that encompassed all 5 NM lightning warning circles on KSC and CCAFS. They were developed using a 15-year (1989–2003) archive of Cloud-to-Ground Lightning Surveillance System (CGLSS) data, 1200 UTC Florida synoptic soundings, and the 1000 UTC CCAFS sounding (XMR). These equations outperformed the operational forecast methods used by the 45 WS. In particular, they outperformed the Neumann-Pfeffer Thunderstorm Index (NPTI) (Neumann 1971) by 48%. They also demonstrated good reliability, an ability to distinguish between non-lightning and lightning days, and improved standard categorical accuracy measures and skill scores over persistence. To facilitate user-friendly interaction with the equations, the AMU created a GUI using Microsoft Excel Visual Basic®. During GUI development, the 45 WS provided comments on the design to ensure it addressed their operational needs. Based on the test results, the GUI and equations were transitioned to operations for the 2005 warm season and replaced the NPTI as the official lightning forecast tool.

In Phase II, the AMU re-created the five logistic regression equations with five modifications:

- Increased the POR from 15 to 17 years (1989–2005),
- Modified the valid area to only include the 5 NM warning circle areas,
- Included the XMR 1000 UTC sounding in determining the flow regime of the day,
- Used a different smoothing function for the daily lightning climatology, and
- Determined the optimal layer for the average relative humidity (RH) candidate predictor.

The Phase II equations outperformed the Phase I equations by 8%, and showed better performance than the Phase I equations in four other tests. As a result, the AMU replaced the Phase I equations in the GUI with the Phase II equations and transitioned it to operations. The Phase II equations are currently being used in operations. In addition to the Excel GUI, Mr. Paul Wahner of Computer Sciences Raytheon (CSR) created a MIDDS GUI to have the same look. This made it easier for forecasters to transition from the Excel to the MIDDS GUI. More importantly, the MIDDS GUI retrieved the required sounding parameter values automatically for the equations. To use the Excel GUI, the forecasters had to gather the sounding values and enter them in the GUI manually. This increased the risk of entering an incorrect value and calculating an erroneous probability. It also increased the time forecasters spent in preparing the daily and weekly forecasts. The MIDDS GUI reduces the possibility of human error and increases efficiency, allowing forecasters to do other duties.

1.2 Phase III

For Phase III, the 45 WS tasked the AMU to update the Phase II equations with three modifications. The first was to increase the POR to 20 years by adding the warm season data from the three years 2006-2008. The daily climatology for the Phase II POR in Figure 1 illustrates the driving factors for the other two modifications. The smoothed values were created with a Gaussian center-weighted function (Lambert 2007). The 14-day smoothed values show the climatologies tapering off through the end of September, but not leveling out as can be seen at the beginning of May. Therefore, the second modification was to add October data to the POR to determine if a climatological end to the lightning season could be found in that month.

The third, and primary, modification was to stratify the data by the progression of the lightning season instead of by month for the equation development. This progression can be seen best in the 14-day smoothed daily climatology values in Figure 1. The values are low and the curve is flat in the first part of May. The curve increases from mid-May to mid- to late-June, where it then plateaus through mid-August. The lightning probability trend then decreases through September. The goal was to stratify the data into "sub seasons" at the inflection points where the trends changed instead of by month, and create an equation for each sub-season. Such stratification could capture the physical properties important to thunderstorm formation within each sub-season, possibly resulting in better-performing equations.

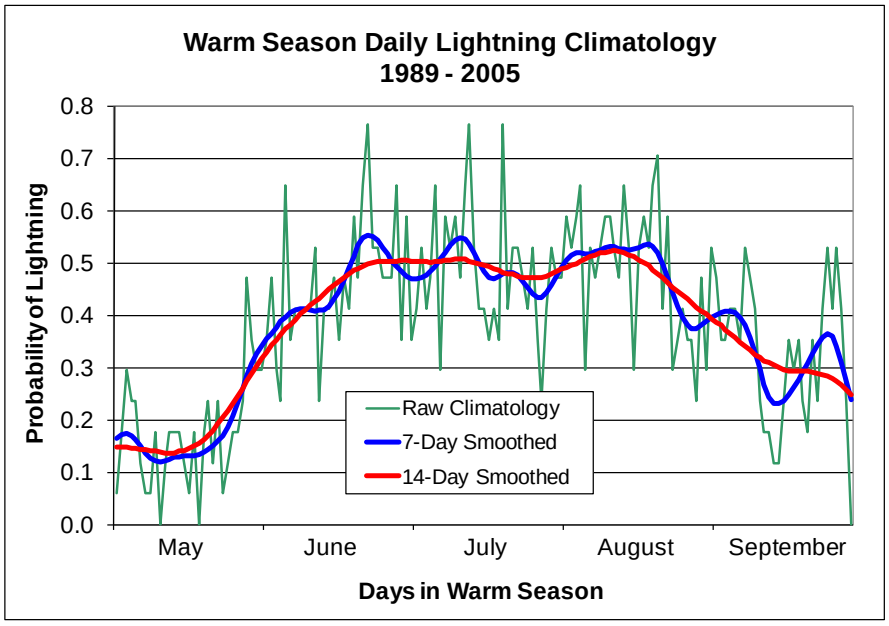

Figure 1. The Phase II daily raw (green), ±7-day smoothed (blue), and ±14-day smoothed (red) climatological probability values of lightning occurrence for the warm season months in 1989–2005.

2 Data

The POR for the data used to develop the forecast equations was increased from 17 to 20 years by adding the data collected during the 2006–2008 warm seasons, and the October data for 1989–2008. The data sources include the

- CGLSS,
- 1200 UTC Jacksonville (JAX), Tampa (TBW), and Miami (MFL) Fla. soundings, and
- 1000 UTC XMR sounding.

Data from CGLSS, the local network of cloud-to-ground lightning sensors, were used to determine lightning occurrence within a defined area (see Section 3.1) for each day. The 1000 UTC XMR and 1200 UTC JAX, TBW, and MFL soundings were used to calculate the daily flow regimes, and the 1000 UTC XMR soundings were used to calculate the standard stability parameters that are readily available to the forecasters. Discussions for each data type used are included in this report for completeness, but only information pertaining to Phase III for brevity. More details on each data type can be found in the Phase I final report (Lambert and Wheeler, 2005).

2.1 CGLSS

The CGLSS is a network of six sensors Figure 2 that collects date/time, latitude/longitude, peak current, and polarity information of cloud-to-ground lightning strikes in the local area. Mr. Steve Madison of CSR provided the additional data for the 2006–2008 warm seasons and the October data. The CGLSS data were used to determine whether or not lightning occurred on each day in the POR. The primary purpose of the CGLSS data was to create the binary predictand for the equations. The data were also used to create the daily climatological lightning frequency and persistence forecasts that would be used as candidate predictors and forecast methods against which to test the new equations.

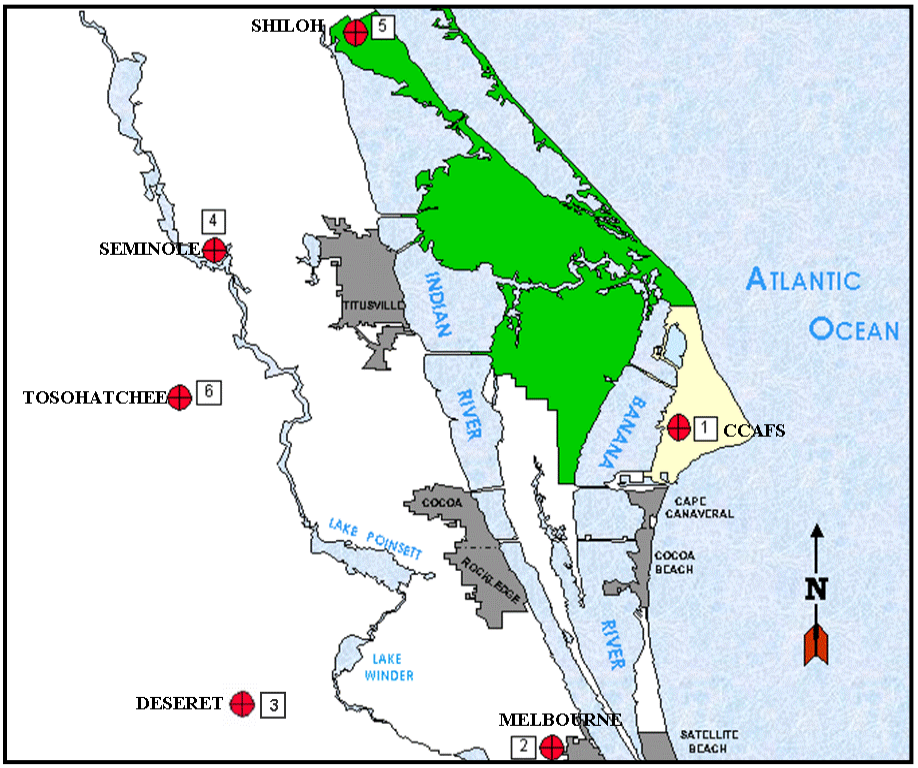

Figure 2. The locations of the six CGLSS sensors are indicated by the red circles. The location names are next to the circles.

2.2 Florida 1200 UTC Soundings

These data were collected to determine the daily flow regimes (Lericos et al. 2002, Lambert 2007). The AMU downloaded sounding data for the 2006–2008 warm seasons and October 1989–2008 from the Global Systems Division/Earth System Research Laboratory web site http://www.esrl.noaa.gov/raobs/. As noted in Lericos et al. (2002), the current MFL and JAX sites were located at West Palm Beach, Fla. (PBI) and Waycross, Ga. (AYS), respectively, prior to 1995. The PBI and AYS data were used as proxies for MFL and JAX, respectively, during the period 1989–1994. All future references to MFL and JAX include the 1989–1994 data from AYS and PBI. The map in Figure 3 shows the locations of all the soundings.

Use of the 1200 UTC sounding may seem inappropriate as it cannot provide data in time for the 1100 UTC briefing. The previous 0000 UTC sounding was ruled out because contamination by afternoon convective circulations could mask the larger scale flow pattern at this time. For the purpose of determining the flow regimes for each day in the POR, the 1200 UTC sounding provided the most reliable data. Due to the weak synoptic patterns during the Florida warm season, it is not likely that a flow regime change would take place in the two-hour period between 1000–1200 UTC. In an operational setting, the 45 WS can use several data sources, including model output and surface observations, to determine the flow regime of the day before the 1100 UTC briefing. Specific suggestions for data sources and procedures that can be used to determine the flow regime are discussed in Section 7.22 in the Phase II final report (Lambert 2007).

2.3 XMR 1000 UTC Soundings

The XMR sounding location is shown in Figure 3. The 45 WS forecasters use data from the 1000 UTC sounding for the 1100 UTC morning briefing since it contains the most recent information on the state of the atmosphere over the area. They were used to supplement the Florida 1200 UTC soundings in determining the flow regime of the day and to calculate the sounding parameters normally available to the forecasters through MIDDS. The probability of lightning occurrence based on flow regime and the XMR sounding parameters were used as candidate predictors in the equation development.

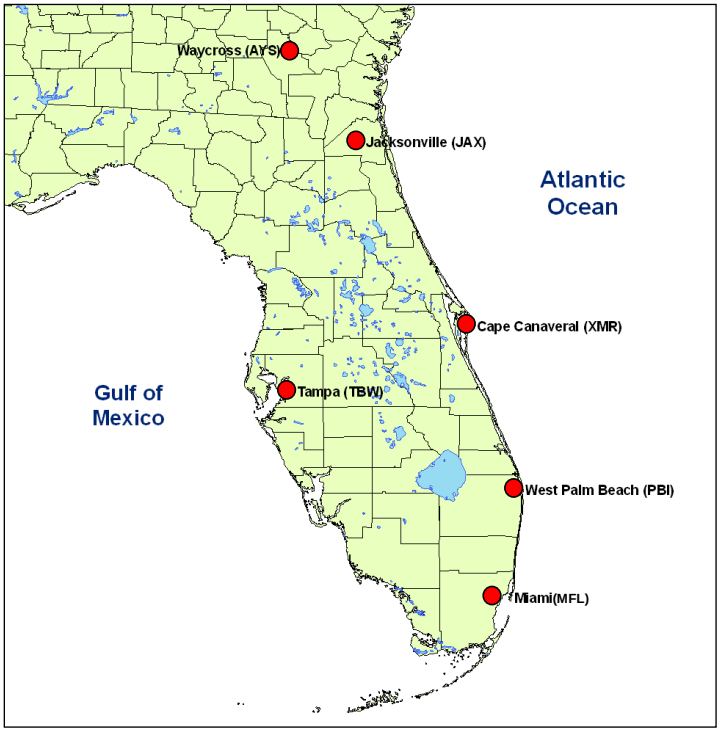

Figure 3. The red dots on the map show the locations of all soundings used in this task.

3 Data Preparation

The AMU processed the three datasets described in Section 2 to create the equation elements needed for the statistical forecast equation development: the predictand and candidate predictors. The predictand is the element to be predicted from a predictor or group of predictors. There was one predictand value and one set of candidate predictor values per day in the POR. More details of how the data were processed to create these elements are given in the Phase II final report (Lambert 2007). All data were processed using the S-PLUS® statistical software package (Insightful Corporation 2007).

3.1 CGLSS

The CGLSS data provided the ground truth of whether or not lightning occurred within the 5 NM circles for which the 45 WS has forecasting responsibility (Figure 4) for each day in the POR. The data were filtered spatially to include only strikes that occurred within these circles, and temporally to include only lightning strikes recorded in the time period 0700–0000 EDT.

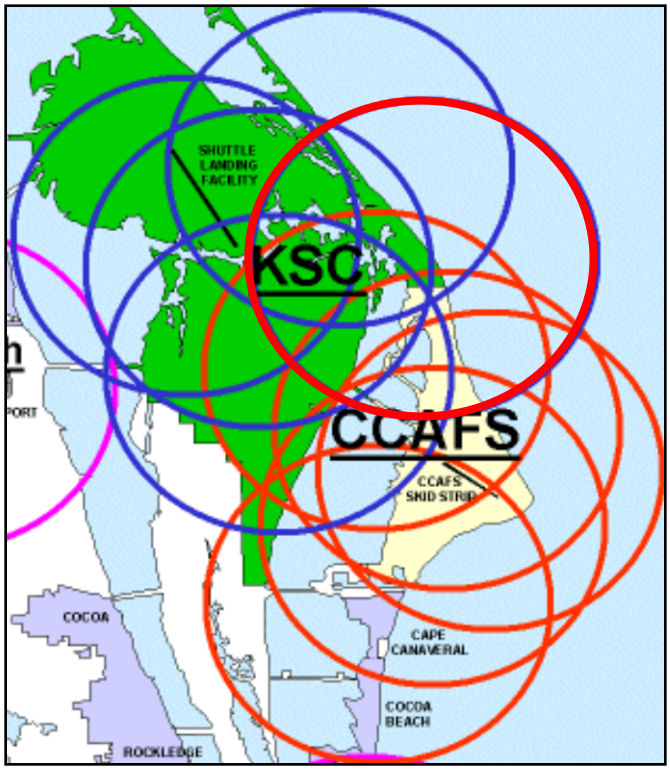

Figure 4. The 5 NM lightning warning circles on KSC/CCAFS. The valid area is within the four blue (KSC) and six red (CCAFS) circles.

The AMU used the filtered CGLSS data to create the predictand as well as the 1-day persistence and daily climatology candidate predictors. The value of the predictand was binary: '1' if one or more strikes were detected within the defined time and space, '0' if no lightning was detected. The 1-day persistence predictor was also binary: If lightning occurred on one day, the persistence value for the next day was '1'. If lightning did not occur, the persistence value was '0'. The predictand values were used to create the daily climatology. Figure 5 shows the raw, 7-day smoothed, and 14-day smoothed daily climatology curves. Details on how the values were calculated are in the Phase II final report (Lambert 2007). As in Phase II, the 14-day smoothed values were used for the daily climatology in the equation development. The new May–October 1989-2008 daily lightning climatology values in Figure 5 were consistent with the previous 1989-2005 climatology (Figure 1), being only ~1% lower on average.

One of the questions to be answered by this work was whether the October data should be included as part of the overall lightning season. Given that the daily values at the beginning of October are higher than those at the beginning of May, the 45 WS and AMU agreed that these data should be included.

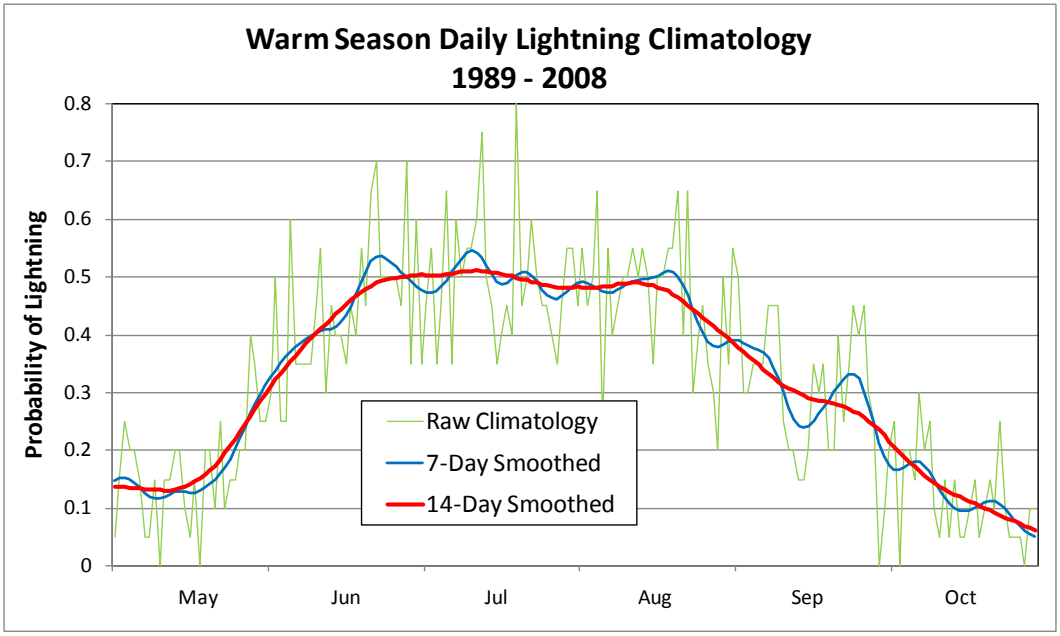

Figure 5. The Phase III daily raw (green curve), ±7-day smoothed (blue curve), and ±14-day smoothed (red curve) climatological probability values of lightning occurrence for the warm-season months including October in 1989–2008.

3.2 Soundings

The AMU used the Florida synoptic and XMR soundings to determine the flow regime of the day. The first step was to determine the synoptic flow regime of the day through a combination of the average 1000–700 mb wind directions from the 1200 UTC MFL, TBW, and JAX soundings, as outlined in Lericos et al. (2002). Table 1 shows the criteria used to determine the daily flow regime. The mathematical procedure used to calculate the average wind direction in the 1000–700 mb layer is in Lambert and Wheeler (2005). The next step was to calculate the average 1000–700 mb wind directions in the 1000 UTC XMR soundings, which were used to determine the 'local' flow regime of the day (Lambert 2007). The local flow regime was used to determine the final flow regime of the day when the synoptic regime was Other, Missing, SE-1, or SW-2. In the SE-1 and SW-2 regimes, the ridge axis from the high over the Atlantic Ocean was just north or south of TBW, respectively. Exactly where the ridge was located relative to KSC/CCAFS was unknown. If the synoptic regime was SE-1 but the local regime showed southwest flow, SE-1 was replaced with SW-2, and vice versa.

The flow regimes were used with the CGLSS predictand to calculate the probability of lightning occurrence for each flow regime in Table 1 within each lightning sub-season to be used as candidate predictors in the equation development. However, a method for determining the sub-season dates had to be developed first. The methods tested for stratifying the data by sub-season are discussed in Section 4.

Table 1. List of the flow regime names used in Phases I and II and the corresponding sectors showing the average 1000 – 700 mb wind directions at each of the stations.

Flow Regime Name and Description		***Rawinsonde Station***		
		MFL	**TBW**	**JAX**
SW-1	Subtropical ridge south of MFL Southwest flow over KSC/CCAFS	180°-270°	180°-270°	180°-270°
SW-2	Subtropical ridge north of MFL, south of TBW Southwest flow over KSC/CCAFS	90°-180°	180°-270°	180°-270°
SE-1	Subtropical ridge north of TBW, south of JAX Southeast flow over KSC/CCAFS	90°-180°	90°-180°	180°-270°
SE-2	Subtropical ridge north of JAX Southeast flow over KSC/CCAFS	90°-180°	90°-180°	90°-180°
NW	Northwest flow over Florida, likely from a stronger-than-average subtropical ridge south of MFL extending into Gulf of Mexico	270°-360°	270°-360°	270°-360°
NE	Northeast flow over Florida, likely from a stronger-than-average subtropical ridge north of JAX extending into southeast U.S., at times forming a closed high pressure center	0°-90°	0°-90°	0°-90°
Other	When the layer-averaged wind directions at the three stations did not fit in defined flow regime			
Missing	One or more soundings missing			

The 1000 UTC XMR soundings were also used to calculate the stability indices normally available to the forecasters through MIDDS. In order to calculate the same values that would be available to the forecasters, the AMU used the same equations as are used in the MIDDS code. All the routines that the AMU developed in Phase I to create the stability indices were used in Phase III.

The stability index candidate predictors included the

- Total Totals,
- Cross Totals,
- Vertical Totals (VT),
- K-Index (KI),
- Lifted Index (LI),
- Thompson Index (TI),
- Severe Weather Threat (SWEAT) Index,
- Showalter Stability Index,
- Temperature at 500 mb (T_{500}),
- Mean RH in the 800–600 mb layer (Avg.86.RH),
- Mean RH in the 825–525 mb layer (Avg.85.RH),
- Precipitable water (PW),
- Mean wind speed in the 1000–700 mb layer, and
- The lapse rate between the 700 and 500 mb levels in °C/km (L57).

The formulas used to calculate the indices are standard and can be found in several sources (e.g. Peppler and Lamb 1989). Five indices in the above list are not readily available to the forecasters: VT, TI, Avg.86.RH, Avg.85.RH, and L57. The TI is calculated easily with the equation TI = KI – LI, as is VT with T_{850} - T_{500}. Avg.86.RH and Avg.85.RH were calculated using a weighted average described in the Phase II final report (Lambert 2007). L57 is the absolute value of $(T_{500} - T_{700})/(Height_{500} - Height_{700})$

3.3 Data for Sub-Season Stratification

Five distinct sub-seasons are evident from the 14-day smoothed curve in Figure 5 (dates are approximate):

1) Pre-lightning 1–13 May,
2) Ramp-up 14 May–22 June,
3) Lightning 23 June–12 August,
4) Ramp-down 13 August–12 October, and
5) Post-lightning 13–31 October.

The actual sub-seasons in different years likely start on different days. To stratify the data properly, the start dates of each sub-season in each individual year should be used. The method to choose the dates would have to be objective and repeatable so that forecasters could use the same procedure in real-time operations. The development and testing of three methods is discussed in Section 4.

3.3.1 Ground-Truth Dates

Determining the accuracy of an objective method to choose sub-season start dates would be difficult without the aid of ground-truth dates. In 2002, the National Weather Service in Melbourne, Fla. (NWS MLB) conducted a study to determine the signatures for the start of the wet and dry seasons (Lascody 2002). Through objective and subjective analysis of several surface and sounding variables, the study determined the start dates for Orlando in the years 1949–2002 and Daytona Beach in the years 1935–2002. The dates have been determined every year since the study ended, and the lists now contain start dates through 2009.

Because of the extensive objective and subjective analysis done, the AMU determined the NWS MLB wet and dry season start dates would be used as ground-truth dates for the lightning and post season start dates, respectively, in each POR year. An objective method developed by the AMU would be considered a success if it was able to choose dates within seven days of these dates. The AMU chose the Daytona Beach dates due to that city's close proximity to the Atlantic Ocean, similar to KSC/CCAFS. Table 2 shows the NWS MLB dates in Month/Day order to show the distribution of start dates regardless of year. The last row in the table shows the median wet and dry season start dates for the Phase III 20-year POR.

Table 2. The NWS MLB wet and dry season start dates for Daytona Beach in the Phase III POR years 1989–2008.

Wet Season Start				***Dry Season Start***			
13 May	1991	2 Jun	2003	27 Sep	2006	16 Oct	2002
19 May	1997	3 Jun	1990	30 Sep	2001	16 Oct	2004
20 May	1995	4 Jun	1989	6 Oct	1992	17 Oct	1994
21 May	1996	6 Jun	2007	7 Oct	1991	18 Oct	1995
27 May	1992	7 Jun	2002	9 Oct	1996	19 Oct	1989
27 May	1999	10 Jun	2008	9 Oct	2000	19 Oct	1997
29 May	1994	11 Jun	2006	12 Oct	1993	22 Oct	1999
30 May	2001	12 Jun	1993	14 Oct	2005	24 Oct	1990
30 May	2005	22 Jun	2000	14 Oct	2008	24 Oct	1998
1 Jun	2004	6 Jul	1998	15 Oct	2003	3 Nov	2007
Median: 2 June				**Median: 16 October**			

3.3.2 Data for Objective Method

Discussions with the NWS MLB and 45 WS forecasters as well as the results from the NWS MLB study indicated that PW might be a good variable to use in determining the start of the sub-seasons. Prior to the AMU calculating the stability indices from the XMR sounding, the 14th Weather Squadron (14 WS) calculated the daily means and standard deviation of PW over the 20-year POR for the 45WS. To compare them with the smoothed daily climatology, the AMU applied the 14-day smoothing algorithm to the PW means and standard deviations. These values and the daily climatology from Figure 5 are shown in Figure 6 along with the start dates of the wet and dry seasons from the NWS MLB study. The last dry season date, 3 November, is not shown in the chart since the x-axis does not go beyond 31 October.

The median wet season start date of 2 June is close to half way along the upward trend in daily climatologies, and the median dry season start date of 16 October is close to where the daily climatology decreases to the same values as at the beginning of the season in early May. The smoothed PW mean values show trends similar to the daily climatology. They peak a few days later in June than the daily climatology values. The plateau of PW means lasts into early September, but the daily climatology values begin to decline in mid-August. A “bump” in values exists in both curves during late September. The smoothed standard deviations are steady throughout the season until toward late September when they steadily increase. The similarities between the curves at the beginning of the warm season indicate that PW may be a good indicator of the beginning of the ramp-up and lightning sub-seasons, but it may not be helpful in determining the beginning of the ramp-down and post-lightning sub-seasons.

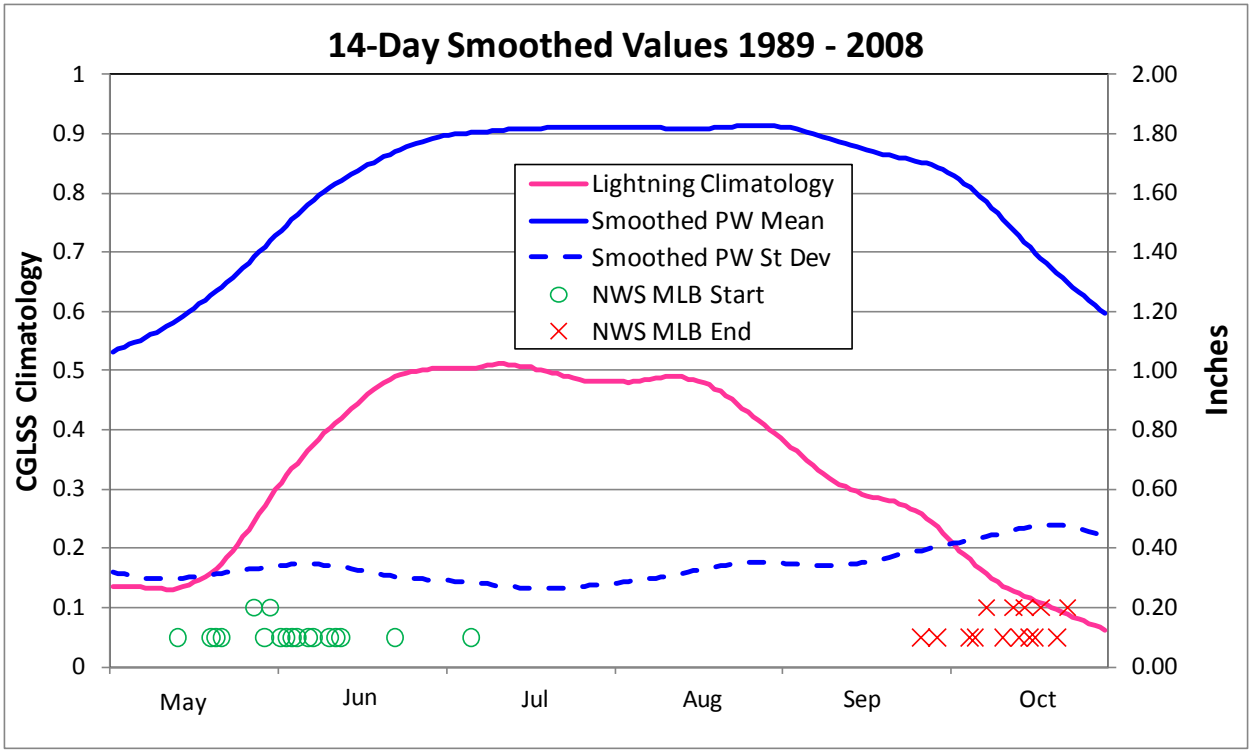

Figure 6. The 14-day Gaussian-smoothed daily climatology from Figure 5 (left axis, magenta line) and 14 WS PW (right axis) means (solid blue line) and standard deviations (dashed blue line) with the NWS MLB wet season start (green circles) and end (red Xs) dates in the POR. The values for the start and end dates are plotted using the vertical axis on the right. A value of 0.1 means the wet season began/ended only once on that date in the POR, and 0.2 means it began/ended on that date twice in different years.

After calculating all the parameters listed in Section 3.2, the AMU analyzed their 20-year means to determine which might be good indicators of sub-season beginning dates, and found that LI, KI, TI, PW, Avg.86.RH and Avg.85.RH showed the most promise. Figure 7 shows the daily 20-year mean values for these parameters. All but LI begin at relatively low values, increase through days 45–50 (14–19 June), plateau through days 145–150 (22–27 September), and then decrease through day 184 (31 October). The LI had opposite and much less pronounced trends. The increase in KI, TI, PW and the two RH values as well as the decrease in LI are consistent with the increase in daily climatology. While the trends at the beginning of the warm season closely match the KSC/CCAFS daily climatology, the decrease for all parameters is approximately a month later than for the daily climatology (Figure 6).

The AMU then analyzed the standard deviations of the mean values in Figure 7, shown in Figure 8. At the beginning of the warm season, the standard deviations of most parameters were only slightly less than, if not equal to, their associated mean. This indicated too much variance in the parameters to make good indicators of lightning sub-season dates. However, the PW standard deviations were 1/3 to 1/4 of their mean values. As the warm season progressed to the lightning sub-season, the standard deviations decreased, but increased again toward the end of the season. Even the PW values became larger toward the end of the warm season. Due to the relatively low standard deviations, PW is a better candidate for discerning the beginning of the ramp-up and lightning sub-seasons. However, the larger standard deviations toward the end of the warm season indicate PW might not be a good discriminator for the beginning of the ramp-down and post-lightning sub-seasons.

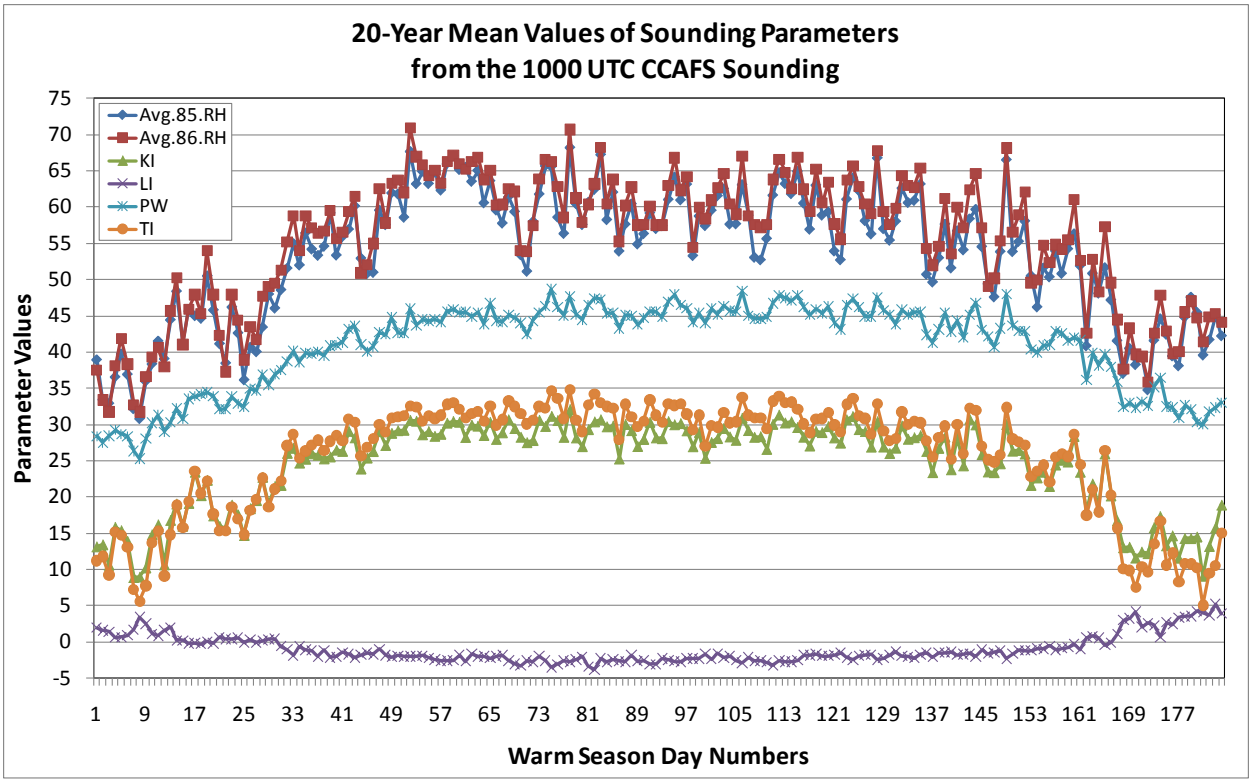

Figure 7. The 20-year daily mean values of Avg.85.RH, Avg.86.RH, KI, LI, PW, and TI. The magnitude of the values is on the vertical axis, and the warm season day numbers, beginning with 1=1 May and ending with 184=31 October, are along the horizontal axis. RH values are in percent and PW values are in mm.

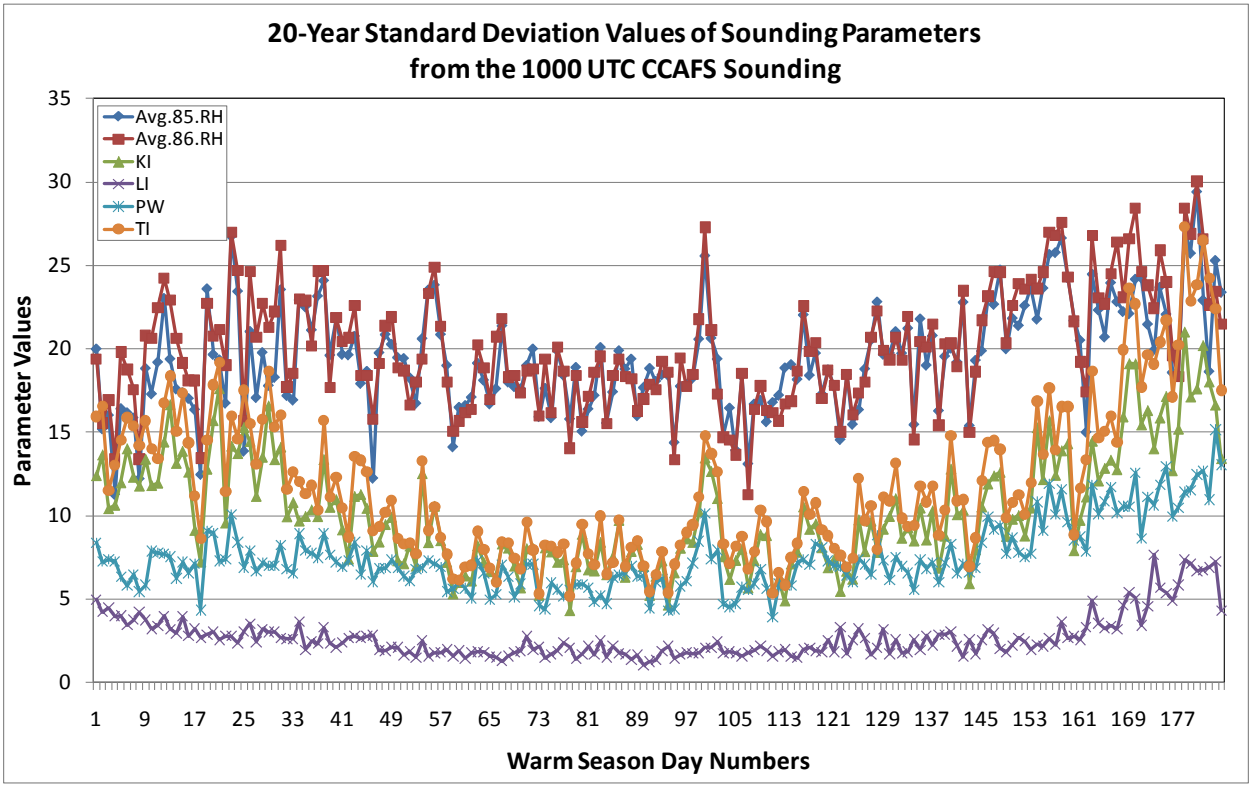

Figure 8. As in Figure 7, but for the 20-year daily standard deviation values.

4 Sub-Season Start Dates

Once all the data were prepared, the AMU began developing and testing methods to determine the beginning dates of the sub-seasons. Given the trends in the PW means and standard deviations in Figure 7 and Figure 8, this was the main parameter used in the development. Also due to the closer association of the PW and daily climatology curves at the beginning of the season and the lower PW standard deviations, the AMU began by developing and testing methods to determine the start of the ramp-up and lightning sub-seasons. If successful, the technique would be extended to determine the start of the ramp-down and post-lightning sub-seasons. Once the start dates could be determined, the flow regime lightning probabilities could be calculated for each sub-season.

The AMU tested three statistical methods to determine which could choose the sub-season start dates:

- Number of occurrences above a PW threshold value from the beginning of the warm season,
- One-Sample t Test on the running PW mean, and
- Multiple discriminant analysis (MDA).

As stated in Section 3.3.1, the NWS MLB dates were used as ground truth in determining the ability of the techniques to identify the start of the lightning sub-season. To be successful, the technique had to choose a date within one week (± 7 days) before or after the NWS MLB date in each year.

4.1 Chronological Check

The first method was a simple chronological check of the number of occurrences of a threshold PW value. Since the daily PW values in any individual year can be highly variable from day to day, especially early in the season, the first occurrence of a threshold value is not likely a good indicator of the start of a sub-season. The AMU created an algorithm that began at Day 1 (1 May) and checked the daily PW values in chronological order. At the point where the daily lightning climatology values start to increase in mid-May, the average PW value is 1.2 in (30.5 mm). At the point where the values begin to plateau in June, it is 1.75 in (44.5 mm).

The start of the ramp-up sub-season was defined reasonably well after the third occurrence of PW ≥ 1.2 in. There is no equivalent ground truth for this date, only the daily lightning climatology. The average start-day for the ramp-up sub-season using this technique was 10 May, only three days earlier than the apparent start-day of 13 May from the daily climatology. The start days ranged from 3 – 19 May over the 20-year POR.

The search for the start of the lightning sub-season began the day after the ramp-up start date. In some years with moist days at the beginning of the season, the ramp-up and lightning start dates were the same if both algorithms began at 1 May. Setting the number of occurrences to three and using a PW threshold of ≥ 1.75 in, the algorithm was only able to choose lightning sub-season start dates within one week of the NWS MLB start dates in 8 of the 20 years. A 40% success rate was not acceptable. In the other 12 years, dates were chosen that were 2 – 3 weeks before or after the NWS MLB wet season start date. The AMU varied the number of occurrences from two to five and the threshold from 1.7–1.8 in, but no combination produced better results.

4.2 One-Sample t Test

The next method tested to determine the start date of the lightning sub-season was the one-sample t test. This test is used to determine if an observed sample mean was drawn from a population with a predetermined mean. The t value is given by the equation

$$t = \frac{\bar{x} - \mu_0}{[\hat{Var}(\bar{x})]^{\frac{1}{2}}},$$

Where in this case $\bar{x}$ is the running PW mean, μ_0 is the predetermined PW threshold to define the start of the lightning sub-season, and $\hat{Var}(\bar{x})$ is the sample estimate of the sample mean variance defined as

$$\hat{Var}(\bar{x}) = {s^2}/{n},$$

where s^2 is the sample variance (s is the standard deviation) and n is the sample size (Wilks 2006). The null hypothesis, H_0, is that $\bar{x}$ is drawn from a population whose mean is μ_0, and the alternative hypothesis is that the mean is not μ_0. For a small value of t, the difference in the numerator is small compared to the variance term in the denominator. If it is more than twice the denominator, H_0 is likely to be rejected (Wilks 2006). S-PLUS has a function for the t Test that outputs the test statistic t and a parameter called the p value. The p value is the probability that t will occur. If $p \leq$ the test level, in this case 5% or 0.05, then H_0 is rejected.

The AMU began testing this method with $\mu_0 = 1.75$ in and $n = 4$ (days). The first day checked in each year was the day after the ramp-up start. The PW from each day plus the three days previous were used to calculate the running mean. If the p value indicated that the running mean was likely$\geq \mu_0$, the fourth day in the running mean was considered the start of the lightning sub-season. The results in comparison with the NWS MLB start dates were worse than the chronological check. Only 6 dates out of 20 were within one week of the NWS MLB dates. The AMU varied the number of days in the running mean (n) from three to eight, μ_0 from 1.7 to 1.8 in, and the number of occurrences from one to three with similar or worse results. The other days not within one week of the ground-truth dates varied from two to three weeks before and after those dates, with no apparent pattern.

4.3 Multiple Discriminant Analysis

MDA is a statistical method used to discern between groups in a dataset. In this case, the AMU used it to discern between the ramp-up and lightning sub-seasons in each year, thereby determining the lightning sub-season start date. The steps in developing an MDA equation are given in Wilks (2006). The AMU used an equivalent function in S-PLUS to develop and test the MDA.

4.3.1 MDA Data and Function

The AMU began by creating the dataset needed to develop the MDA function. This dataset contained the year, month, day, PW, KI, LI, and TI for all dates in the POR, and a group parameter that identified whether the day was in the ramp-up or lightning sub-season. The NWS MLB wet-season start dates were the beginning points for the lightning sub-season in each year, and the ramp-up start dates were those chosen by the chronological check described in Section 4.1. The end of the lightning sub-season also had to be chosen so the development data contained only days from the ramp-up and lightning sub-seasons. This was estimated from the daily climatology in Figure 5 and Figure 6 to be 15 August in every year. This was the date just before the downward trend in lightning frequency. Data from the odd years in the POR were used for the MDA development, and the resulting function was first tested on the development data. It is a good test of a predictive function to use the data from which it was developed. If it does not perform well with the development data, it will not perform well with other data.

The MDA function has the form

$$V = C_1x_1 + C_2x_2 \ldots + C_nx_n,$$

where V is the value used to determine the group classification (ramp-up or lightning), C_n are the constant coefficients for the data values, x_n are the variable values, and n is the number of variables used in the MDA function. The coefficients are determined through complex matrix algebra using the variables and the group parameter in the development data set. The classification between two groups depends on whether V is greater or less than a dividing point value, determined by using the mean values of the variables in the development data set for $x_1 \ldots x_n$ in the equation above. An MDA function was developed using all the data in the development data set combined, then tested on each individual year in that data set. The S-PLUS function automatically assigned a group classification to each day.

4.3.2 MDA Development and Testing

The AMU first used PW alone as the variable to develop the MDA (n = 1). This function performed poorly when tested with the development data, especially in years that were moist at the beginning of ramp-up or with dry spells in the ramp-up and lightning seasons. Ramp-up days were usually identified well at the start of that sub-season through mid-May, and lightning sub-season days were identified consistently usually starting in late June/early July. In the period between, the classifications for consecutive days became mixed such that no clear pattern or threshold point for the start of lightning season could be discerned.

One parameter is usually not enough to forecast thunderstorm development with accuracy. The moisture represented by PW is critical, but instability is also needed. Therefore, the AMU added TI (n = 1,2) to the development, where TI = KI – LI: KI accounts for low-level moisture and lapse rate, and LI accounts for the low- to mid-level instability. The mean seasonal curve of TI had the same relation to lightning frequency as did PW (Figure 7). Even though the standard deviation of TI was high during May, it began decreasing in June and may be a good lightning sub-season discriminator when combined with PW. Indeed, when tested on the development data, the period of mixed classifications spanning the late ramp-up and early lightning sub-seasons decreased as compared to using only PW. Also, the number of successive days classified as lightning increased toward the end of the "mixed" period, interspersed with fewer and fewer successive days classified as ramp-up.

Using a pattern of three days in a row with a lighting classification, the AMU was able to identify the beginning of the lightning sub-season within one week of the NWS MLB dates in 5 of the 10 odd years used to develop the MDA, and using four days in a row identified 4 of the 10 years. This was encouraging, but considering the MDA was tested on the data from which it was developed, this performance was not acceptable. Figure 9 shows the PW and TI values for the ramp-up (blue Xs) and lightning (red squares) sub-season days. Note the large overlap of the two sub-season groups highlighted by the red box between PW=20–40 and TI=0–35. For MDA to be effective, there must be a more clear separation of the groups.

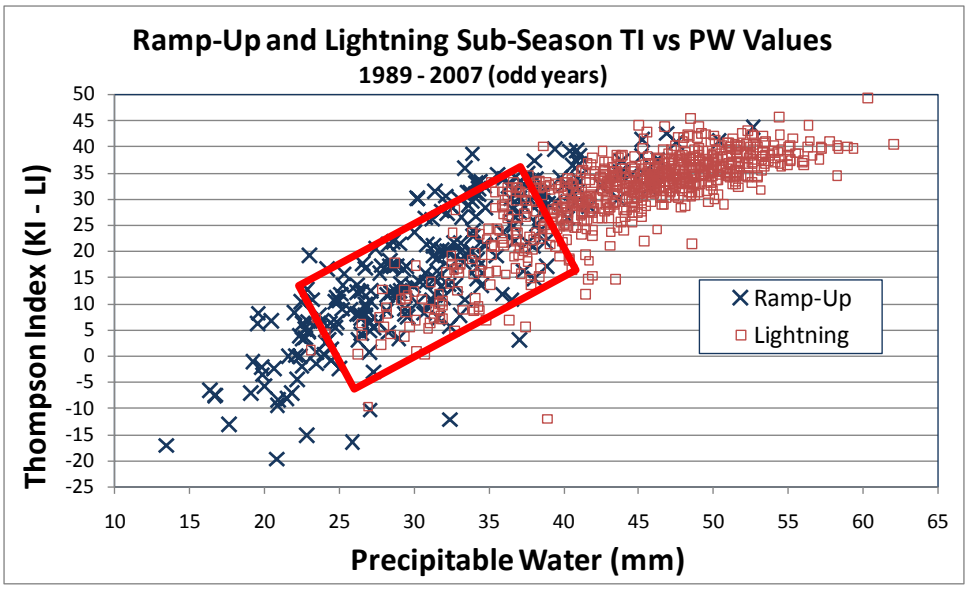

Figure 9. Scatter diagram of TI vs PW values for the ramp-up (blue Xs) and lightning (red boxes) sub-seasons for the odd years in 1989–2007. The red box surrounds the area of overlap between ramp-up and lightning sub-season days.

4.4 Daily Climatology

While not successful, the MDA method showed promise as a sub-season discriminator and should be explored in future work. However, due to time constraints on the task, the AMU and 45 WS agreed to end testing methods that would determine the sub-season start dates in each individual year and, instead, define the dates using the daily lightning climatology. The black Xs in Figure 10 show the beginning of each sub-season:

- Ramp-up begins 18 May when the climatological lightning frequency starts to increase;
- Lightning begins 6 June, the point at which the rate of increase in the frequencies begins to decrease and just four days later than the median NWS MLB wet season start date;
- Ramp-down begins 17 August when the large decrease in lightning frequency begins; and
- Post begins 12 October when the rate of decrease lessens and becomes steady and the value reaches 0.13, the same as in the pre-lightning sub-season.

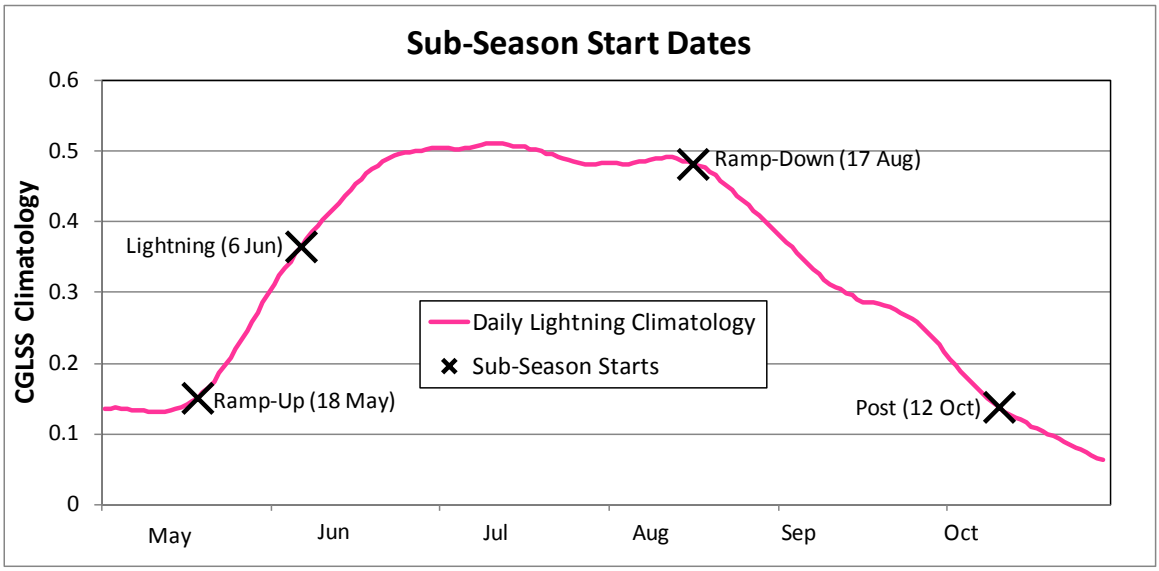

Figure 10. The 1989 – 2008 daily lightning climatology with the sub-season start dates indicated by black Xs.

The lightning sub-season start date appears out of place on the curve in Figure 10. The AMU and Mr. Roeder of the 45 WS discussed several methods for choosing this date. The probability values begin to plateau at≥ 0.48 on 23 June, which was the original start date of choice for the lightning sub-season. However, this date was later than the 90th quartile of the NWS MLB wet season start dates. They decided to determine the point at which the increase in probabilities began to decrease and use that date as the start-date for the lightning sub-season. This occurred on 6 June, just four days after the NWS MLB mean wet season start date of 2 June.

4.5 Flow Regime Lightning Probabilities

As stated earlier, the data had to be stratified into sub-seasons before the flow regime lightning probabilities could be calculated. The AMU stratified the data in each year into sub-seasons by the dates in Figure 10 and created flow regime lightning probabilities for each sub-season. A detailed description of the procedure to calculate these values is given in the Phase II final report (Lambert 2007). These probabilities were used as a candidate predictor in the equation development and are shown in Table 3. The values for the SW-1/SW-2 and for the SE-1/SE-2 regimes calculated separately were within 10% of each other. Therefore, the SW-1/SW-2 days and SE-1/SE-2 days were combined to increase the sample size and produce a more reliable probability value.

Table 3. Sub-season probabilities of lightning occurrence in percent based on the flow regimes. The values in the far-right column are the sub-seasonal probabilities for all flow regimes combined.

Sub-Season	SW-1/2	SE-1/2	NW	NE	Other	Monthly
Pre-Lightning	23	13	10	4	4	13
Ramp-Up	42	13	28	3	22	25
Lightning	67	31	51	13	42	48
Ramp-Down	54	32	17	14	28	32
Post-Season	28	5	1	6	5	9

5 Equation Development and Testing

There were three major steps in this portion of the task:

- Ascertain data availability,
- Develop the logistic regression equations, and
- Determine the equation performance.

The amount of data available for equation development was critical to the reliability of the new equations. After determining that an appropriate amount of data was available, a set of five equations was developed, one for each month in the warm season. The performance of the equations was assessed using several verification techniques appropriate for probability forecasts.

5.1 Data Availability

The amount of available data was determined before equation development began. This was important since the data had to be stratified into development and verification datasets followed by stratification into sub-season datasets, thereby limiting the amount of data available for equation development. To ensure the new equations would be reliable, ample data were required to create realistic relationships between the predictors and the predictand. The World Meteorological Organization (1992, hereafter WMO) states that there should be at least 250 events in the dataset in order to derive stable statistical relationships. This was the threshold in determining whether there were sufficient data.

5.1.1 Missing Data

There are 184 days in the warm season for this task, 1 May–31 October. This equates to 3680 days over the 20-year POR. Sounding data were not available every day. Data were considered missing for a specific day if one or more of the 1200 UTC Florida synoptic soundings (MFL, TBW, JAX) and the 1000 UTC XMR sounding were missing to determine the flow regime, or when a 1000 UTC XMR sounding was missing to calculate the stability parameters. Table 4 shows the number of days in each sub-season, how many of those days had missing data, which dataset was missing, and the total number of days with available data. There were few cases in which data were missing from both datasets on the same day. The number in the third column under the heading "# MISSING DAYS" in Table 4 is less than the sum of the first two columns in every case because there were a few days in which data were missing from both datasets. The numbers of overlap cases are shown in parentheses in the third column. The last column in Table 4 shows that data availability ranged from 89–93% for each sub-season, and 90% overall.

Table 4. Summary of available data in the POR. The first column contains the names of the sub-seasons, where Total is for the entire season. The two columns under "# POSSIBLE DAYS" show the number of days in 1 and 20 seasons. The three columns under "# MISSING DAYS" show the number of unavailable days due to missing data from each dataset in the subheadings, and the number of days missing combined from both datasets. The value in parentheses in the third column is the number of days in which data were missing from both datasets. The final column shows the number of days with all data available. The percent of total possible days is given in parentheses.

Sub-Seasons	# POSSIBLE DAYS		# MISSING DAYS			Total Available (% of # Possible)
	1 Year	20 Years	MFL TBW JAX XMR	XMR	Total (Overlap)	
Pre-Lightning	17	340	6	23	26 (3)	314 (92)
Ramp-Up	19	380	9	23	27 (5)	353 (93)
Lightning	72	1440	35	122	143 (14)	1297 (90)
Ramp-Down	56	1120	15	105	115 (5)	1005 (90)
Post-Lightning	20	400	7	45	46 (6)	354 (89)
Total	**184**	**3680**	**72**	**318**	**357 (33)**	**3323 (90)**

5.1.2 Development and Verification Datasets

The development dataset required enough samples so that the resulting set of equations was stable, i.e. the equations would maintain consistent forecast accuracy on different datasets. The verification dataset was needed for equation testing in order to have a more realistic view of how the equations would perform in operations. It was expected that the equations would not perform as well on the verification data as they would on the data from which they were developed. However, if performance were a great deal worse with the verification data, this would indicate that either too many predictors were chosen and the equations were fit too strongly to the development data, or the development dataset was too small.

The candidate predictors and predictand for each sub-season were stratified into development and verification datasets. Care was taken to ensure there would be at least 250 events in the development dataset, while still having enough events in the verification dataset to make reasonable conclusions about equation performance. Of the 20 seasons in the POR, 16 were used for equation development and 4 were set aside for equation verification.

The stratification did not involve choosing whole warm season years for each dataset, but rather individual warm season days. Days for the verification dataset were chosen first. Given that there are 184 days in the warm season, the random number generator in Microsoft Excel was used to create four sets of 184 numbers representing the years 1989 to 2008. The four sets of years were assigned to each day. Thus, each day in the warm season was represented by days from four random years. This ensured that each day was equally represented in the verification and development datasets. Care was taken to ensure the there were no duplicate years for each day from the random number generator. For example, the verification dataset contains 1 May 1996/2001/2004/2008, …, 31 October 1997/2003/2006/2007. All other dates were made part of the development dataset. This random method ensured that any abnormal convective season would not skew the development of the equations or their verification. Table 5 shows the possible number of events for the development and verification datasets and the actual number after accounting for missing data. Note the number of days in the development dataset for each month in the right-most column. All are above the 250 event threshold defined by the WMO needed to develop reliable equations.

Table 5. Summary of available data. The first column contains the name of each sub-season, where Total is for the entire season. The three columns under "# POSSIBLE DAYS" show the number of days in 20 warm seasons, the number of days for equation verification, and the number for development. The three columns under "# AVAILABLE DAYS", show the number of days actually available in the POR due to missing data (Table 4), and the actual number of days for verification and development.

Sub-Seasons	# POSSIBLE DAYS			# AVAILABLE DAYS		
	Total	**Verification**	**Development**	**Total**	**Verification**	**Development**
Pre-Lightning	340	68	272	314	62	252
Ramp-Up	380	76	304	353	66	287
Lightning	1440	228	1212	1297	267	1030
Ramp-Down	1120	224	896	1005	197	808
Post-Lightning	400	80	320	354	73	281
Total	**3680**	**676**	**3004**	**3323**	**665**	**2658**

5.2 Equation Development

As in Phases I and II, logistic regression was used to create five equations, except for each sub-season in this case instead of each month. Predictor selection was conducted for each individual sub-season to account for the possibility that different variables may be more critical to convection formation as the season progresses. Detailed descriptions of logistic regression and the predictor selection procedure with supporting figures and equations are found in the Phase II final report (Lambert 2007). For the sake of brevity, these descriptions will not be repeated in this report since the procedures were followed exactly for this task.

The AMU developed and tested several versions of each equation, each with varying numbers of predictors. The version that performed best on the verification data set was chosen as the final equation. Table 6 shows the predictors for each of the sub-season equations in rank order of their importance in predicting lightning. The predictor names are color-coded to highlight their occurrence in each equation. Blue identifies TI, which was chosen as the most important predictor in the first four sub-seasons. Red identifies the flow regime lightning probabilities. This parameter was the second predictor chosen in the ramp-up, lightning, and ramp-down sub-seasons, and the most important predictor in the post-lightning sub-season. Persistence is in green and was chosen as the third predictor for the ramp-up and lightning sub-seasons. VT and LI were used only once as the last predictors for the ramp-down and post-lightning sub-seasons, respectively. The first predictor in the first four equations, TI, accounts for instability and moisture in the profile, which are both necessary ingredients for thunderstorm formation. The flow regime probability accounts for the lifting mechanism, or lack thereof, from the low-level flow interacting with the sea breeze front, which occurs almost daily in the warm season.

Table 6. The final predictors for each sub-season equation, in rank order of their importance in predicting lightning occurrence. Predictor names are colorized to highlight their occurrence in each equation. Vertical Totals and Lifted Index are in black font since they were only used once.

Pre-Lightning	***Ramp-Up***	***Lightning***	***Ramp-Down***	***Post-Lightning***
Thompson Index	Thompson Index Flow Regime Persistence	Thompson Index Flow Regime Persistence	Thompson Index Flow Regime Vertical Totals	Flow Regime Lifted Index

5.3 Equation Performance

The predictors from the four-warm-season verification dataset were used in the Phase II and III equations to produce 'forecast' probabilities. Using the verification dataset provided an independent assessment of equation performance that could be used to conclude how the equations will perform in future operations. The forecast probabilities were compared with the binary lightning observations in the verification dataset using the Brier Skill Score, which is a measure of equation performance versus other forecast methods, in this case Phase III performance over Phase II. If Phase III outperformed Phase II, other tests to determine reliability and skill would be conducted. Otherwise, testing would cease and the Phase III equations would not be transitioned into operations.

5.3.1 Phase II and III Forecast Probabilities

The Phase II equation forecasts were used as a benchmark to determine if the Phase III equations improved the forecast. In Phase II, an equation was developed for each month, May–September. In order for the equations to perform as they currently do in operations and perform a fair comparison with the Phase III equations, the verification data were stratified by month for the probability calculations, excluding October. The Phase II flow regime probabilities were also calculated for each month and were different than those in Table 3. Therefore, the flow regime values from Phase II were used in the Phase II equations. Care was taken to make sure the flow regime probability values matched the correct flow regime day in the verification data. Once all the probabilities were calculated for each month, the values were appended to create a non-stratified full season dataset, and then re-stratified into the sub-seasons described in Section 4.4 for comparison with the Phase III probabilities.

The Phase III probabilities were calculated for all sub-seasons, May – October. The performance of the post-lightning sub-season equation could not be compared to the Phase II equations since there was not an October equation from that work. The ramp-down season was compared, but only using data through the end of September even though the equation development included data through 11 October. This caused 39 days out of 197 (~20%) in the ramp-up verification dataset to be excluded from the comparison.

5.3.2 Brier Skill Scores

The Brier Skill Scores were calculated for each individual sub-season to show how each equation performed against four standard forecast methods and the Phase II equations. The number of available days in each month of the verification data ranged from 62–267 (Table 5). The pre-lightning, ramp-up, and post-lightning sub-season samples were small, but large enough to provide a reasonable estimate of relative skill with the Brier Skill Score. The five forecast methods were

- 1-day persistence,
- Daily climatology (Figure 10),
- Flow regime probabilities (Table 3),
- Sub-seasonal probabilities (percent of days lightning occurred), and
- Phase II equation probabilities.

The AMU began by first calculating the mean squared error (MSE) between the forecasts and observations for all six forecast methods using the equation

$$\mathrm{MSE} = \frac{1}{n}\sum_{i=1}^{n}(p_i - o_i)^2 \text{ (Wilks 2006),}$$

where n is the number of forecast/observation pairs, p_i is the probability associated with the forecast method, and o_i is the corresponding binary lightning observation. The skill of the Phase III equations over the five forecast methods was calculated using the Brier Skill Score (SS) equation:

$$\mathrm{SS} = \left(\frac{\mathrm{MSE}_{\mathrm{eqn}} - \mathrm{MSE}_{\mathrm{ref}}}{\mathrm{MSE}_{\mathrm{perfect}} - \mathrm{MSE}_{\mathrm{ref}}}\right)*100 \text{ (Wilks 2006),}$$

where MSE_{eqn} was the MSE of the Phase III equations, MSE_{ref} was the forecast method against which the equations were tested, and $MSE_{perfect}$ was the MSE of a perfect forecast, which is always 0. The SS represents a percent improvement or degradation in skill of the equation over the reference forecast when it is positive or negative, respectively.

The SS values for each of the Phase III equations and a composite result for the entire warm season are shown in Table 7. The Phase III equations show a double-digit improvement in skill for most of the first four methods in the table, except for the 7% improvement over the flow regime probabilities in the pre-lightning and lightning sub-seasons. Of the first four methods, the smallest percent improvements were over the probabilities based on flow regime. The excellent performance of the Phase III equations over the first four methods did not foretell the dismal performance against the Phase II equations. In no sub-season did the Phase III equations outperform the Phase II equations, although the degradation in performance for the lightning sub-season was small if not insignificant.

Table 7. The percent (%) improvement or degradation (red font) in skill of the Phase III over the Phase II equations and other standard forecast methods using the verification data.

Forecast Method	***Pre-Ltg***	***Ramp-Up***	***Lightning***	***Ramp-Dn***	***Post-Ltg***	***Season***
Persistence	52	48	51	47	57	50
Daily Climatology	17	18	25	23	23	23
Sub-Season Climatology	18	22	25	27	21	31
Flow Regime	7	13	7	15	18	11
Phase II Equations	-12	-12	-0.6	-4.1	—	-3.6

The degradation in skill of the Phase III equations could have several causes. The development datasets for the pre-lightning and ramp-up seasons had just enough samples to meet the WMO criteria, but had fewer samples than the monthly datasets in Phase II, which ranged from 368–404 samples (Lambert 2007). More cases may result in better predictor selection and coefficient calculation for the logistic regression. However, the lightning and ramp-down sub-seasons had 1030 and 808 samples in their development datasets and the equations were still under-performers. The data were not stratified by sub-season start dates in each individual year, but the same start dates were used in every year. It's highly likely that this wholesale method of choosing start dates resulted in some days being chosen for a particular sub-season that were actually part of the sub-season before or after. As a result, the predictor values would not all be representative of the sub-season. This could cause different predictors to be chosen and would certainly affect the value of the coefficients of the predictors in the equation.

Regardless of the cause, the Phase III equations produced a degradation in skill and will not be transitioned to operations. This also dictated that no more testing of Phase III equation performance would be conducted.

6 Summary and Recommendations

The AMU created new logistic regression equations in an effort to increase the skill of the Objective Lightning Forecast Tool developed in Phase II (Lambert 2007). One equation was created for each of five sub-seasons based on the daily lightning climatology instead of by month as was done in Phase II. The assumption was that these equations would capture the physical attributes that contribute to thunderstorm formation more so than monthly equations. However, the SS values in Section 5.3.2 showed that the Phase III equations had worse skill than the Phase II equations and, therefore, will not be transitioned into operations. The current Objective Lightning Forecast Tool developed in Phase II will continue to be used operationally in MIDDS.

Three warm seasons were added to the Phase II dataset to increase the POR from 17 to 20 years (1989–2008), and data for October were included since the daily climatology showed lightning occurrence extending into that month. None of the three methods tested to determine the start of the sub-season in each individual year were able to discern the start dates with consistent accuracy. Therefore, the start dates were determined by the daily climatology shown in Figure 10 and were the same in every year.

The procedures used to create the predictors and develop the equations were identical to those in Phase II. The equations were made up of one to three predictors. TI and the flow regime probabilities were the top predictors followed by 1-day persistence, then VT and LI. Each equation outperformed four other forecast methods by 7–57% using the verification dataset, but the new equations were outperformed by the Phase II equations in every sub-season. The reason for the degradation may be due to the fact that the same sub-season start dates were used in every year. It is likely there was overlap of sub-season days at the beginning and end of each defined sub-season in each individual year, which could very well affect equation performance.

6.1 Predictor Comments

The candidate predictors used to develop the equations were the same as those in Phase II with two additions: the mean speed in the 1000–700 mb layer and L57 (lapse rate between 700 and 500 mb). These two were added because the 45 WS forecasters found them to be important in forecasting thunderstorms and lightning over KSC/CCAFS. Also, the 850 and 500 mb wind speeds were important predictors in the previously-operational Neumann-Pfeffer Thunderstorm Index (Pfeffer 1967). Throughout the statistical predictor selection process, neither of these predictors was chosen as important to lightning occurrence, and indeed were among the least important predictors, mathematically speaking. This result was surprising to those that make the lightning forecast. They find that strong or weak flow will either pin convection to the coast, allow the sea breeze to penetrate inland slowly, or force the sea breeze to penetrate inland early before storms can start. This is critical for the placement of thunderstorms and, therefore, lightning. For the 2010 warm season, L57 proved to be an important predictor. PW was abundant, but the lack of instability did not support thunderstorm formation at KSC/CCAFS.

The equations were developed using data from 16 warm seasons and the predictors chosen were those that were important for lightning occurrence most of the time, not just in special cases. It does not mean that wind speed or L57 are not important and should not be considered on any given day. The output from this tool can be considered a climatological probability and should be considered a first-guess in developing the daily lightning probability, not the final value. Forecasters should look at wind speed, L57, the other candidate predictors, other observations, and model data to determine the final lightning probability for the day.

6.2 Suggested Future Work

Future work could include a task to create new monthly equations that include October since the daily climatology developed in this task showed it to contain significant lightning probabilities. Since lightning probability forecasts for May are provided in the current tool, probabilities for October should also be provided given that the values in early October were higher than those in early May. Also, in any individual October, the lightning season could extend past the early part of the month. This would be a relatively easy task since the procedures developed in the previous phases would be followed, the only difference being the addition of data from seasons that pass between now and the beginning of the work.

Future work should include an effort to create an objective method that determines the sub-season start dates in each individual year. The inability to do that in this task is likely the reason for the degraded performance of the equations. MDA showed promise as a method to do this, and other statistical methods could be tested. While the forecasters could determine the current lightning sub-season subjectively, an objective technique to identify the sub-season is needed to develop and verify the sub-season equations. It would be time-consuming to identify the sub-season after it has begun subjectively since it requires analyzing lightning events across Florida and other weather data over several days in real-time. One way to objectively identify lightning sub-seasons would be to examine lightning data from across Florida and determine a threshold of number of flashes, perhaps over a number of consecutive days, or large change in flashes during a range of dates. Such a dataset would be very large and time-consuming to analyze. The time-consuming nature of conducting a subjective analysis to determine the sub-season start dates makes the development of an objective method the desired approach.

Finally, any future work should continue to consider L57 and the 1000–700 mb layer wind speed as candidate predictors. As stated in Section 6.1, the forecasters consider these values to be very important predictors of lighting occurrence in the KSC/CCAFS area. The forecasters should be consulted at the beginning of the work for other candidate predictors not listed in this report so a thorough assessment of the importance of each can be made. Consultation with the forecasters prior to and during the development of the equations is critical to the success of the tool as they have the experience to know what is important in lightning forecasting.

References

Bauman, W. H., W. P. Roeder, R. A. Lafosse, D. W. Sharp, and F. J. Merceret, 2004: The Applied Meteorology Unit – Operational Contributions to Spaceport Canaveral. Preprints, 11th Conference on Aviation, Range, and Aerospace Meteorology, Amer. Meteor. Soc., Hyannis, MA, 4-8 October 2004, 24 pp.

Insightful Corporation, 2007: *S-PLUS 8 for Windows User's Guide*, Insightful Corp., Seattle, WA, 584 pp.

Lambert, W., 2007: Objective Lightning Probability Forecasting for Kennedy Space Center and Cape Canaveral Air Force Station, Phase II, NASA Contractor Report CR-2007-214732, Kennedy Space Center, FL, 59 pp. [Available from ENSCO, Inc., 1980 N. Atlantic Ave., Suite 830, Cocoa Beach, FL 32931, and online at http://science.ksc.nasa.gov/amu/final.html].

Lambert, W. and M. Wheeler, 2005: Objective lightning probability forecasting for Kennedy Space Center and Cape Canaveral Air Force Station. NASA Contractor Report CR-2005-212564, Kennedy Space Center, FL, 54 pp. [Available from ENSCO, Inc., 1980 N. Atlantic Ave., Suite 830, Cocoa Beach, FL, 32931, and online at http://science.ksc.nasa.gov/amu/final.html].

Lascody, R., 2002: The Onset of the Wet and Dry Seasons in East Central Florida - A Subtropical Wet-Dry Climate? NWS Melbourne, FL, http://www.srh.noaa.gov/mlb/?n=wetdryseason.

Lericos, T., H. Fuelberg, A. Watson, and R. Holle, 2002: Warm season lightning distributions over the Florida Peninsula as related to synoptic patterns. *Wea. Forecasting*, **17**, 83 – 98.

Neumann, C. J., 1971: Thunderstorm forecasting at Cape Kennedy, Florida, utilizing multiple regression techniques. NOAA Technical Memorandum NWS SOS-8.

Peppler, R. A. and P. J. Lamb, 1989: Tropospheric static stability and Central North American growing season rainfall. *Mon. Wea. Rev.*, **117**, 1156 – 1180.

Pfeffer, G. C., 1967: Objective thunderstorm forecasting technique for Patrick AFB and Cape Kennedy AFS.

Wilks, D. S., 2006: *Statistical Methods in the Atmospheric Sciences*. 2d ed. Academic Press, Inc., San Diego, CA, 467 pp.

World Meteorological Association (WMO), 1992: *Methods of Interpreting Numerical Weather Prediction Output for Aeronautical Meteorology*. Technical Note No. 195, ISBN 92-63-10770-X, 89 pp.

List of Acronyms

14 WS	14th Weather Squadron
45 WS	45th Weather Squadron
AMU	Applied Meteorology Unit
Avg.85.RH	Mean RH in the 825-525 mb layer
Avg.86.RH	Mean RH in the 800-600 mb layer
AYS	Waycross, Ga. 3-letter identifier
CCAFS	Cape Canaveral Air Force Station
CGLSS	Cloud-to-Ground Lightning Surveillance System
CSR	Computer Sciences Raytheon
GUI	Graphical User Interface
JAX	Jacksonville, FL 3-letter identifier
KI	K-Index
KSC	Kennedy Space Center
L57	Lapse rate between 700–500 mb
LI	Lifted Index
MDA	Multiple Discriminant Analysis
MFL	Miami, Fla. 3-letter identifier
MIDDS	Meteorological Interactive Data Display System
MSE	Mean Squared Error
NE	Northeast flow regime
NPTI	Neumann-Pfeffer Thunderstorm Index
NW	Northwest flow regime
NWS MLB	National Weather Service Melbourne, Fla.
PBI	West Palm Beach, Fla. 3-letter identifier
POR	Period of Record
PW	Precipitable Water
RH	Relative Humidity
SE	Southeast flow regime
SS	Skill Score
SW	Southwest flow regime
SWEAT	Severe Weather Threat Index
T_{500}	Temperature at 500 mb
TBW	Tampa, FL 3-letter identifier
TI	Thompson Index
VT	Vertical Totals
WMO	World Meteorological Organization
XMR	CCAFS rawinsonde 3-letter identifier

NOTICE

Mention of a copyrighted, trademarked or proprietary product, service, or document does not constitute endorsement thereof by the author, ENSCO Inc., the AMU, the National Aeronautics and Space Administration, or the United States Government. Any such mention is solely for the purpose of fully informing the reader of the resources used to conduct the work reported herein.